Received: 21 October 2019 | Revised: 6 April 2020 | Accepted: 11 May 2020

DOI: 10.1002/ijc.33123

TUMOR IMMUNOLOGY AND MICROENVIRONMENT

IJC International Journal of Cancer

Distinct immune evasion in APOBEC-enriched, HPV-negative HNSCC

Clemens Messerschmidt[1,2] | Benedikt Obermayer[1,2] | Konrad Klinghammer[3] | Sebastian Ochsenreither[3,4,5] | Denise Treue[6] | Albrecht Stenzinger[5,7] | Hanno Glimm[5,8,9] | Stefan Fröhling[5,10] | Thomas Kindler[5,11,12] | Christian H. Brandts[5,13,14] | Klaus Schulze-Osthoff[5,15] | Wilko Weichert[5,16] | Ingeborg Tinhofer[5,17] | Frederick Klauschen[5,6] | Ulrich Keilholz[4,5] | Dieter Beule[1,2,18] | Damian T. Rieke[3,4,19]

[1]Core Unit Bioinformatics, Berlin Institute of Health (BIH), Berlin, Germany

[2]Charité – Universitätsmedizin Berlin, Corporate Member of Freie Universität Berlin, Humboldt-Universität zu Berlin, and Berlin Institute of Health, Berlin, Germany

[3]Department of Hematology and Oncology, Campus Benjamin Franklin, Charité – Universitätsmedizin Berlin, Corporate Member of Freie Universität Berlin, Humboldt-Universität zu Berlin, and Berlin Institute of Health, Hindenburgdamm 30, Berlin, 12203, Germany

[4]Charité Comprehensive Cancer Center, Charité – Universitätsmedizin Berlin, Corporate Member of Freie Universität Berlin, Humboldt-Universität zu Berlin, and Berlin Institute of Health, Berlin, Germany

[5]German Cancer Consortium (DKTK) and German Cancer Research Center (DKFZ), Heidelberg, Germany

[6]Institute of Pathology, Charité – Universitätsmedizin Berlin, Corporate Member of Freie Universität Berlin, Humboldt-Universität zu Berlin, and Berlin Institute of Health, Berlin, Germany

[7]Institute of Pathology, Heidelberg University Hospital, Heidelberg, Germany

[8]Department of Translational Medical Oncology, National Center for Tumor Diseases (NCT) Dresden and German Cancer Research Center (DKFZ), Dresden, Germany

[9]University Hospital Carl Gustav Carus, Technische Universität Dresden, Dresden, Germany

[10]Department of Translational Medical Oncology, National Center for Tumor Diseases (NCT) Heidelberg and German Cancer Research Center (DKFZ), Heidelberg, Germany

[11]Department of Hematology, Medical Oncology & Pneumology, University Medical Center, Mainz, Germany

[12]University Cancer Center Mainz (UCT), Johannes Gutenberg-University, Mainz, Germany

[13]University Cancer Center Frankfurt (UCT), Goethe University Frankfurt, Frankfurt, Germany

[14]Department of Medicine, Hematology/Oncology, Goethe University, Frankfurt, Germany

[15]Interfaculty Institute of Biochemistry, Tübingen University, Tübingen, Germany

[16]Institute of Pathology, Technical University Munich, Munich, Germany

[17]Department of Radiooncology and Radiotherapy, Charité – Universitätsmedizin Berlin, Corporate Member of Freie Universität Berlin, Humboldt-Universität zu Berlin, and Berlin Institute of Health, Berlin, Germany

[18]Max Delbrück Center for Molecular Medicine in the Helmholtz Association, Berlin, Germany

[19]Berlin Institute of Health (BIH), Berlin, Germany

Abbreviations: APOBEC, apolipoprotein B mRNA editing enzyme, catalytic polypeptide-like; BLCA, urothelial bladder carcinoma; CDKN2A, cyclin-dependent kinase inhibitor 2A; CRISPR, clustered regularly interspaced short palindromic repeats; CTLA4, cytotoxic T-lymphocyte-associated protein 4; DKTK MASTER, Deutsches Konsortium für translationale Krebsforschung Molecular aided stratification for tumor eradication research; DNA, deoxyribonucleic acid; ECOG, eastern co-operative oncology group; GDC, genomic data commons; HLA-A, human leukocyte antigen A; HNSCC, head and neck squamous cell carcinoma; HPV, human papilloma virus; ICI, immune checkpoint inhibition; IFNG, interferon gamma; LAG3, lymphocyte-activation gene 3; LSCC, lung squamous cell carcinoma; LUAD, lung adenocarcinoma; PDCD1, Programmed cell death protein 1; PD-L1, programmed cell death 1 ligand 1; RNA, ribonucleic acid; SBS, single base substitution; SNV, single nucleotide variation; SYCP2, synaptonemal complex protein 2; TCGA, the cancer genome atlas; t-SNE, t-distributed stochastic neighbor embedding; VAF, variant allele frequency; VTCN1, V-set domain-containing T-cell activation inhibitor 1.

Correspondence
Dieter Beule, Core Unit Bioinformatics, Berlin Institute of Health, Charitéplatz 1, 10117 Berlin, Germany.
Email: dieter.beule@bihealth.de and Damian T. Rieke, Charité Comprehensive Cancer Center, Charitéplatz 1, 10117 Berlin, Germany.
Email: damian.rieke@charite.de

Funding information
Berliner Krebsgesellschaft e.V.; Deutsches Konsortium für translationale Krebsforschung (DKTK)

Abstract

Immune checkpoint inhibition leads to response in some patients with head and neck squamous cell carcinoma (HNSCC). Robust biomarkers are lacking to date. We analyzed viral status, gene expression signatures, mutational load and mutational signatures in whole exome and RNA-sequencing data of the HNSCC TCGA dataset (n = 496) and a validation set (DKTK MASTER cohort, n = 10). Public single-cell gene expression data from 17 HPV-negative HNSCC were separately reanalyzed. APOBEC3-associated TCW motif mutations but not total single nucleotide variant burden were significantly associated with inflammation. This association was restricted to HPV-negative HNSCC samples. An APOBEC-enriched, HPV-negative subgroup was identified, that showed higher T-cell inflammation and immune checkpoint expression, as well as expression of APOBEC3 genes. Mutations in immune-evasion pathways were also enriched in these tumors. Analysis of single-cell sequencing data identified expression of APOBEC3B and 3C genes in malignant cells. We identified an APOBEC-enriched subgroup of HPV-negative HNSCC with a distinct immunogenic phenotype, potentially mediating response to immunotherapy.

KEYWORDS
immune checkpoint inhibition, head and neck cancer, APOBEC, mutational signature, tumor inflammation

1 | INTRODUCTION

Cancer is a disease of the genome in that cancer cells have acquired somatic variants that prove advantageous for their growth. These mutations lead to changes in affected proteins and eventually cellular transformation. Altered proteins can be recognized by the immune system through presentation of peptides by the major histocompatibility complex (MHC), which allows for eradication of the tumor. Immune evasion is therefore considered one of the hallmarks of cancer.[1] Immune checkpoint inhibitors (ICI), improving immune recognition and T-cell activation, are an effective treatment option in a subgroup of patients in several cancer types including head and neck squamous cell carcinoma (HNSCC).[2] The presence of an interferon-gamma inflamed gene expression signature (IFNG signature or T-cell inflamed phenotype[3,4]), expression of immune checkpoint PD-L1[2] and tumor mutational burden are associated with response.[5,6] However, effective predictive biomarkers to guide ICI treatment in the clinic are lacking to date.

HNSCC is a common cancer type worldwide. It is mainly caused by tobacco and alcohol consumption, as well as infection with the human papilloma virus (HPV).[7] These two groups (HPV-positive and HPV-negative) are distinct entities with different outcome and different tumor biology.[8] A better responsiveness of HPV-associated tumors to ICI has been suggested by early clinical data[3] but not confirmed in other studies.[2,9] Immune activation due to immunological "foreignness" in virally induced cancers is a potential mechanism of differential immune activation.[10] Additionally, an intracellular antiviral response mediated by the APOBEC3-family of proteins leads to the accumulation of mutations and tumorigenesis.[11] In several cancer types, APOBEC-mediated tumorigenesis is increasingly recognized as an important mechanism, even when independent of viral infections.[12,13] APOBEC activity can be inferred from an analysis of mutational signatures in the tumor genome. A so-called TCW motif has been identified as an APOBEC-specific mutational signature.[14] The role of APOBEC-induced mutations in HPV-negative HNSCC and its

What's new?

Head and neck squamous cell carcinoma (HNSCC) is sometimes susceptible to immune checkpoint inhibitors, and biomarkers are needed to help identify which tumors are most likely to respond. Using the Cancer Genome Atlas, these authors evaluated 496 HSNCCs by HPV status, gene expression signatures, mutational load, and mutational signatures. They found that increased inflammation was associated with APOBEC3-induced mutations in HPV-negative cancers. This newly identified APOBEC-enriched, HPV-negative subgroup showed higher immune checkpoint expression, and also more mutations in immune-evasion pathways, suggesting this may be a way to identify candidates for immune checkpoint inhibitor therapy.

association with immune activation is unclear. We analyzed mutational signatures to uncover mechanisms driving tumor inflammation in HNSCC.

2 | MATERIALS AND METHODS

2.1 | TCGA datasets

TCGA mutation data sets were downloaded for HNSCC[15] (n = 502), lung adenocarcinoma[16] (LUAD, n = 542), urothelial bladder carcinoma[17] (BLCA, n = 395) and lung squamous cell carcinoma[18] (LUSCC, n = 178) from BROAD firehose in MAF format.

2.2 | Identification of an APOBEC-induced subgroup and APOBEC mutational signature

Somatic mutation data in a MAF file was split into separate VCF files, one per TCGA sample. To annotate putative APOBEC induced mutations, we used the method described by Roberts et al,[19] annotating C>T and C>G variants in TCW (TCA, TCT) motifs and their reverse complements, respectively. The number of cytosine mutations in the TCW motif and outside of it in each sample were compared to the respective occurrences of C/G and the TCW motif on chr1 of the human genome with Fisher's exact test.

Values of *P* were subsequently Holm-Bonferroni corrected and all cases with $P' < .05$ were labeled APOBEC-enriched.

COSMIC single base substitution (SBS) signature contributions for the mutational profile of each tumor sample were downloaded from msignaturedb.[20] Samples were grouped and a Wilcoxon rank test was used to test for differences between groups.

2.3 | HPV status

HPV status was assigned based on the number of reads mapping to HPV genomes, which are included as separate contigs in the bam files (genome release 38) available from GDC Portal. We used a cutoff of 3500 reads to label a sample as HPV-positive. Results were checked against the HPV expression signature described by Buitrago-Pérez et al[21] and a derived reduced signature containing only gene CDKN2A and SYCP2 as well as prior results by Tang et al[22] and TCGA clinical annotation for consistency.

2.4 | Expression data analysis and IFNG signature

Expression data for sets of genes ("RNA Seq V2 RSEM") was downloaded from the HNSCC TCGA provisional cohort[15] from cbioPortal.org.[23] Samples that lacked either mutational or expression data were excluded. The IFNG signature was computed as the mean of the log2-transformed RSEM v2 expression values per sample.

2.5 | Identification of gene expression subtypes

HNSCC samples were attributed to gene expression subtypes. Basal, Classical and Inflamed/Mesenchymal cluster centroids were downloaded from the supplementary material of Keck et al.[8] Normalized RSEM expression values from TCGA were log2-transformed and scaled. The nearest centroid in terms of Euclidean distance was then assigned as the label of a sample. To test for independence of variables between Keck classes and APOBEC groups Fisher's exact test was used.

2.6 | Immune population metagene analysis

Gene expression signatures, also called metagenes, for tumor-infiltrating immune populations were acquired from The Cancer Immunome Database[24] (TCIA.at). Enrichment of signatures was computed for each immune population in each sample with the R package GSVA using the method gsva[25]. Differential metagene expression was assessed with limma.[26]

2.7 | Analysis of immunotherapy-essential genes

We analyzed mutations in 554 genes which have been shown to be essential for cancer immunotherapy in a CRISPR assay.[27] To identify enrichment of mutations in these genes, we used a Fisher exact test considering the number of cases in HPV-negative/APOBEC-enriched and HPV-negative/APOBEC-negative respectively, and the number of mutated genes from the aforementioned gene set in each group. Variant effect was annotated with Jannovar.[28]

2.8 | Analysis of APOBEC timing

Variant allele fractions (VAF) of TCW mutations compared to all other variants were used to infer the timing of APOBEC activity. Patients harboring significantly distinct variant allele fractions for TCW variants compared to all other variants of a given case were classified as early APOBEC activation, if the TCW variants had higher VAF, or as late activation, if they had lower overall VAF compared to all other variants. Patients with no difference or too few variants were grouped as "no preference". The false-positive rate was controlled with the R package *q* value,[29] using a threshold of 0.2.

2.9 | Single-cell expression

This analysis was based on the digital expression matrix, holding the expression values of 23 686 genes for 5902 cells of 17 tumor samples (GSE103322), together with a classification into malignant and various nonmalignant cell types provided by the authors.[30] Data were projected into tSNE coordinates using the standard Seurat workflow[31] and visualized using feature plots and violin plots.

2.10 | Independent validation of IFNG signature scores

Patients with advanced cancers, an ECOG performance status of 0–1 and an age < 50 years were eligible for enrollment in the DKTK-MASTER program across cancer centers in Germany. The DKTK-MASTER trial was approved by local ethics committees (Heidelberg and Berlin). Written informed consent was obtained from all participating patients. Whole-exome and RNA sequencing were performed on fresh-frozen tissues. From RNA-seq data for all cases, HPV status was predicted as described above. IFNG signature was computed as described above after generating transcript abundances with salmon[32] against ENSEMBL v75. The mapping of gene symbols used and their respective ENSEMBL ids are shown in Table S1.

3 | RESULTS

3.1 | Identification of inflammation-associated mutational signatures

Mutation and gene expression data from head and neck squamous cell carcinoma samples were downloaded from The Cancer Genome Atlas (n = 496). The presence of a T-cell inflamed microenvironment was

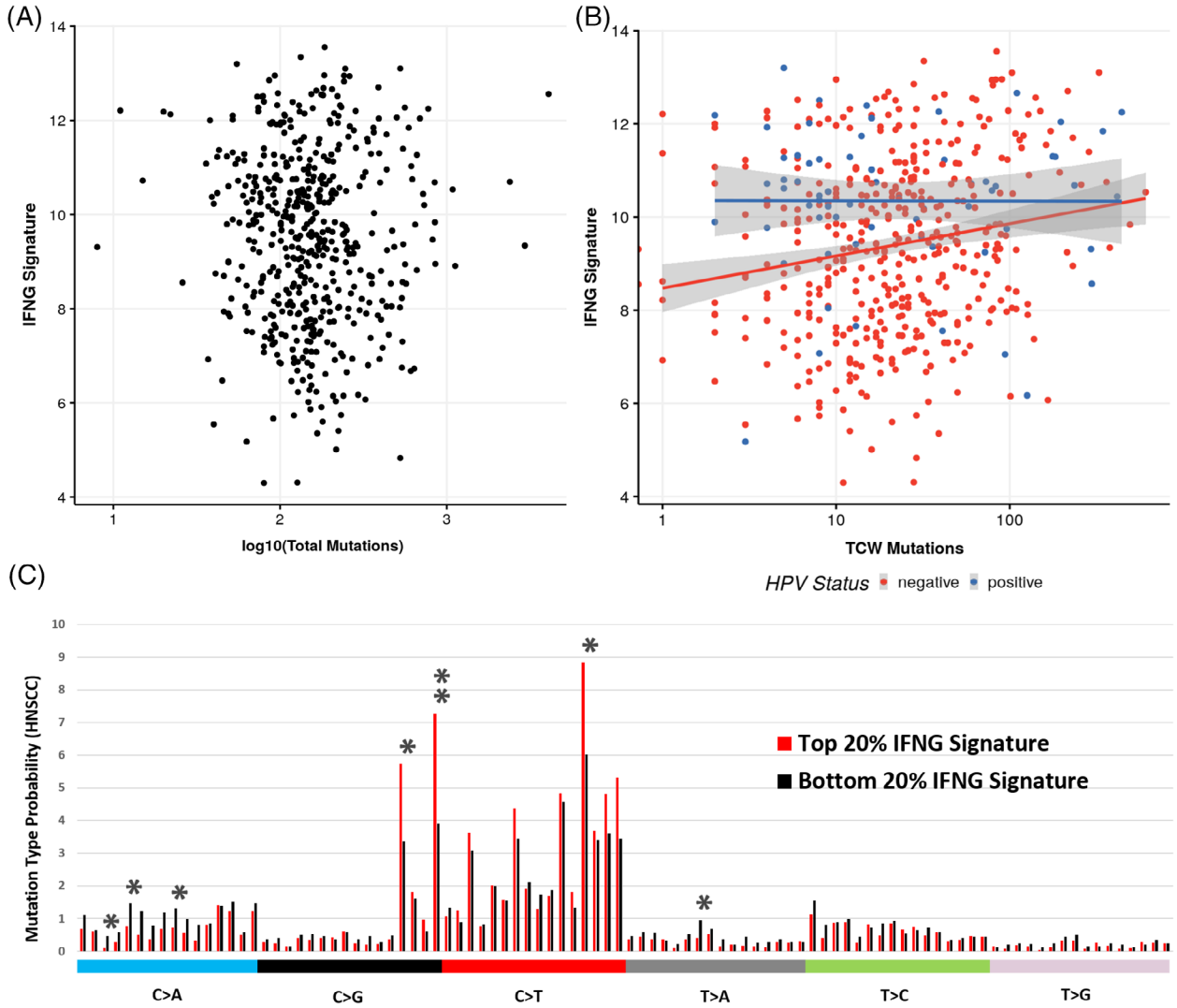

FIGURE 1 Inflammation as measured by an Interferon-gamma signature score is associated with APOBEC activity, not total variant count. A, Relationship between total single nucleotide variant count and the six-gene IFNG signature. No significant correlation was found between these measures ($R = -0.03 \pm 0.08$). B, Relationship between the six-gene IFNG signature and the number of C>T and C>G mutations in TCW motifs. Colors indicate HPV-status (red: HPV-negative, n = 432, blue: HPV-positive, n = 64). A significant correlation between TCW mutations and the IFNG signature was identified in HPV negative cases (R = 0.18, P = 1 × 10−4). C, The frequency of base exchange motifs (eg, C>A substitution with incorporation of the bases at the 5′ and 3′ end, thus allowing 96 potential mutation types) was compared between the patients with the highest and lowest IFNG signature within the TCGA cohort. The top 20% of inflamed cases showed a significant enrichment of variants in the APOBEC3-associated TCW context (*P < .05, **P < .01, all P values were Bonferroni corrected) [Color figure can be viewed at wileyonlinelibrary.com]

assessed in the samples by analysis of a six-gene IFNG signature.[33] Total count of single nucleotide variants (SNV) did not correlate significantly with the IFNG signature (Figure 1A). Next, we analyzed associations between the T-cell inflamed gene expression phenotype and mutational signatures. C>T and C>G mutations are referred to as TCW mutations, as they preferentially occur in TCA and TCT contexts (TCW motif), indicating APOBEC3-induced mutagenesis. TCW mutations were significantly enriched in patients with high expression of the IFNG signature (Figure 1C).

3.2 | Analysis of HPV-status on inflammation and mutational signatures

HNSCC consists of biologically distinct HPV-positive and -negative subgroups. We identified 64 HPV-positive (53 HPV16, 8 HPV33 and 3 HPV35) and 432 HPV-negative samples in the TCGA dataset.

IFNG signature score, total SNV count, counts of TCW mutations and the ratio of the number of TCW mutations compared to the number of total mutations (TCW ratio) were assessed in both groups. Mutational load was significantly more pronounced in HPV-negative samples than in HPV-positive (Figure 2A, $P = 1.7 \times 10^{-4}$), whereas the IFNG signature was significantly higher in HPV-positive samples (Figure 2B, $P = 3.7 \times 10^{-5}$). Further, we compared the ratio of the number of TCW mutations/number of total mutations as a surrogate measure for APOBEC3 mutational activity, which was significantly higher in HPV-positive tumors (Figure 2C, $P = 2.6 \times 10^{-3}$). We then analyzed the association between TCW mutations and inflammation in HPV-positive and HPV-negative HNSCC and found a significant correlation only among HPV-negative HNSCC (Figure 1B). An association between APOBEC-induced TCW-mutations and the IFNG signature could be validated in independent LSCC, LUAD and BLCA datasets (Figure S1).

3.3 | Identification of an APOBEC-enriched HPV-negative subgroup

Since the association between APOBEC-induced mutations (TCW mutations) and the T-cell inflamed phenotype was restricted to HPV-negative samples, we grouped the HPV-negative samples into APOBEC-enriched (n = 84) and APOBEC-negative (n = 348) cases. This newly defined HPV-negative, APOBEC-enriched subgroup showed a higher relative contribution for both APOBEC-associated mutational Signatures 2 and 13 (Figure S2A). Further, the scores of Signatures 2 and 13 ranked higher in the APOBEC-enriched group when compared among the other COSMIC SBS signatures per sample (Figure S2B).

We observed that the HPV-negative subgroup with an enrichment of APOBEC-induced mutations showed a significantly higher IFNG signature score compared to all other HPV-negative cases (HPV-negative, APOBEC-negative; Figure 3A). To exclude the possibility that this signal came from samples falsely classified as HPV-negative, we repeated the analysis by removing all HPV-negative cases with more than five reads mapping to any of the HPV contigs without a change in results (Figure S4).

In addition to differences observed regarding overall inflammation, HPV-negative, APOBEC-enriched cases also exhibited higher predicted infiltration of myeloid-derived suppressor cells (MDSC), Type 17T-helper cell and effector memory CD8+-cell gene expression signatures (Figure S5). Further, differential expression of immune checkpoints was analyzed between groups. A significantly higher gene expression was identified for CD274 (PD-L1), CTLA4, LAG3 and PDCD1 (PD-1) in APOBEC-enriched cases. Only VTCN1 showed a significantly lower gene expression in APOBEC-enriched cases (Figure 3B).

Previous analyses have established different HNSCC subgroups based on gene expression.[8] The APOBEC-enriched HPV-negative samples were assigned to these subgroups and were significantly enriched in the inflamed/mesenchymal cluster (Table S2).

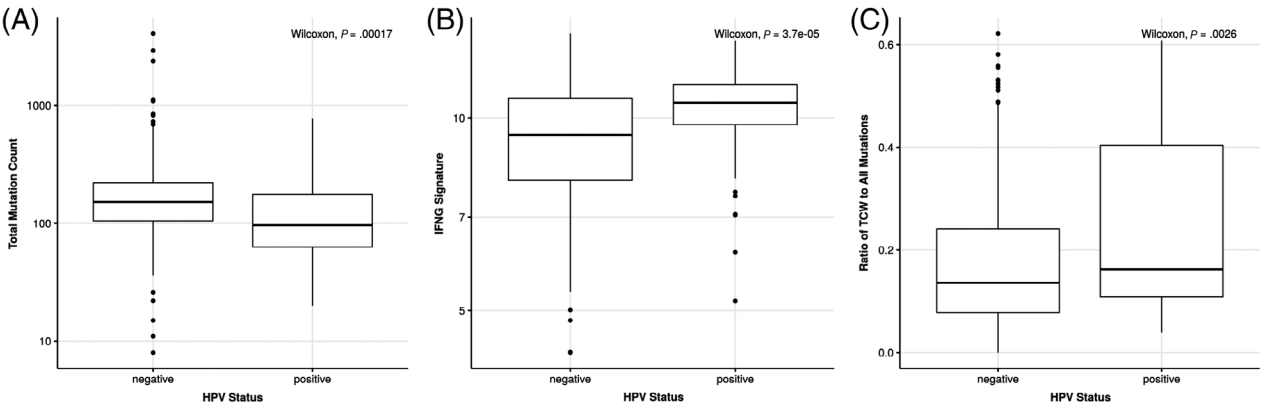

FIGURE 2 HPV status is an important variable in HNSCC. A, Boxplot of total single nucleotide variant count, grouped by HPV status. Total single nucleotide variant count was significantly higher in HPV-negative cases ($P = 1.7 \times 10^{-4}$). B, Boxplot of INFG signature score, grouped by HPV status. The six-gene IFNG signature score was significantly higher in HPV-positive samples ($P = 3.7 \times 10^{-5}$). C, Boxplot of ratio of TCW variants to total single nucleotide variant count, grouped by HPV status. The TCW-ratio was significantly higher in HPV-positive samples ($P = 2.6 \times 10^{-3}$)

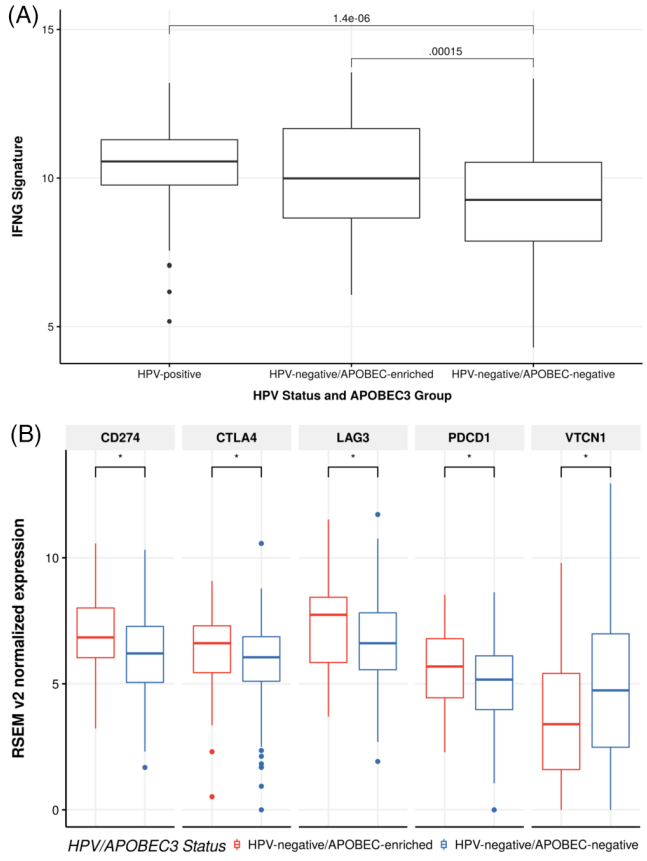

FIGURE 3 HPV-negative, APOBEC-enriched tumors exhibit higher inflammation, higher immune checkpoint expression. A, IFNG signature scores, grouped by HPV status and APOBEC enrichment for HPV-negative cases. HPV negative, APOBEC-enriched HNSCC showed a significantly higher IFNG signature than APOBEC-negative samples ($P = 1.5 \times 10^{-4}$). No significant difference between HPV-positive and HPV-negative/APOBEC-enriched samples was found. B, Gene expression of five immune checkpoints was significantly different between APOBEC-enriched and APOBEC-negative HPV-negative samples ($P' < .05$ after Benjamini-Hochberg correction). All but VTCN1 showed significantly higher expression among APOBEC-enriched cases [Color figure can be viewed at wileyonlinelibrary.com]

We additionally analyzed mutations in immunotherapy-relevant genes.[27] The APOBEC-enriched subgroup showed significantly more variants with functional impact in immunotherapy-essential genes (Table 1, $P = 1.8 \times 10^{-4}$). Among those genes, HLA-A showed the highest relative enrichment among APOBEC-enriched cases and remained significant after correcting for multiple testing (Table S3).

Among HPV-negative samples, smokers were significantly underrepresented ($P = .02$, Table S4) in the APOBEC-enriched group, no significant differences were observed for alcohol consumption. Further, we observe nonrandom associations between tumor site and HPV/APOBEC group ($P < .05$, Table S5) with an enrichment of APOBEC-associated cases in tumor arising from the oral cavity and alveolar ridge but an underrepresentation of laryngeal tumors and tumors of the oral tongue. No difference in overall survival was identified between HPV-negative APOBEC-enriched and APOBEC-negative groups (Figure S3).

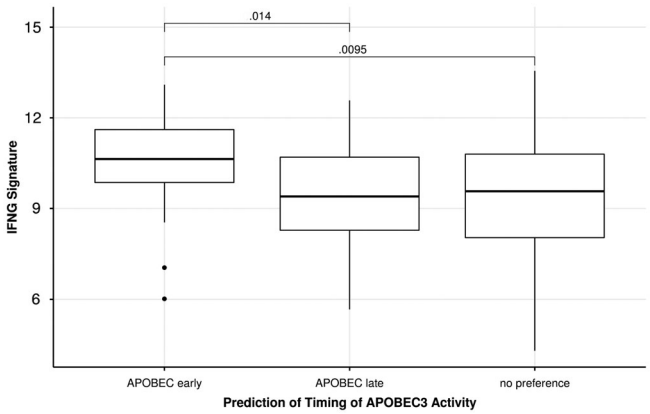

FIGURE 4 Cases with early APOBEC-activation show higher inflammation. IFNG signature score in HPV-negative cases for each group of APOBEC3 activity timing. n (APOBEC early) = 15, n (APOBEC late) = 50, n (no preference) = 367

TABLE 1 HPV-negative APOBEC-enriched and APOBEC-negative groups with counts of hits in gene set identified by Patel et al

	HPV-negative/APOBEC-enriched	HPV-negative/APOBEC-negative	*P* value
No. of cases	84	348	
No. of hits (collapsed to genes)/No. of cases	7.6 (638 total)	4.7 (1643 total)	1.8E−4
No. of hits with functional impact (collapsed to genes)/No. of cases	5.7 (476 total)	3.7 (1277 total)	8.8E−4
No. of hits (collapsed to genes), without HLA genes/No. of cases	7.3 (617 total)	4.7 (1623 total)	4.1E−4
No. of hits with functional impact (collapsed to genes), without HLA genes/No. of cases	5.5 (461 total)	3.6 (1259 total)	1.6E−3

Note: Two sets of Fisher exact tests were carried out, first considering a gene mutated if any variant was found. Second, only mutations with putative functional impact (MODERATE, HIGH flags as returned by Jannovar, eg, missense or stop gain variants) were considered. Both times, the APOBEC-enriched group showed a significant enrichment for mutations in immunotherapy related genes compared to the APOBEC-negative group. Tests were re-done without variants in HLA genes to exclude possible false-positive calls from variant calling.

3.4 | APOBEC activation is an early event in some HNSCC

To identify temporal patterns of APOBEC activation during tumor evolution, we analyzed the variant allele frequency (VAF) of TCW mutations in HNSCC. Cases with early TCW variants exhibited a significantly higher IFNG signature score compared to late TCW activation (Figure 4). We repeated the analysis for the TCGA cohorts of BLCA and LUAD. For BLCA, we did not observe any difference between the groups. However, in LUAD, we observed the opposite effect. Cases with early APOBEC activation were found to exhibit lower inflammation scores than the other two groups, which has been described before[34] (Figure S6).

3.5 | Identification of APOBEC3B and APOBEC3C expression in HNSCC

Gene expression of APOBEC3 family genes was analyzed in the TCGA cohort. HPV-positive samples exhibited significantly higher total APOBEC3 gene expression than HPV-negative samples (Figure 5A). Among HPV-negative samples, the APOBEC-enriched subgroup showed significantly higher expression of APOBEC genes than the APOBEC-negative subgroup. When analyzing APOBEC gene expression by gene, APOBEC3A was most prominently overexpressed in HPV-negative, APOBEC-enriched samples (Figure S7). Since bulk gene expression analyses do not differentiate between tumor and stroma, we analyzed gene expression data in single-cell transcriptome data of HPV-negative HNSCC[30] (GSE103322).

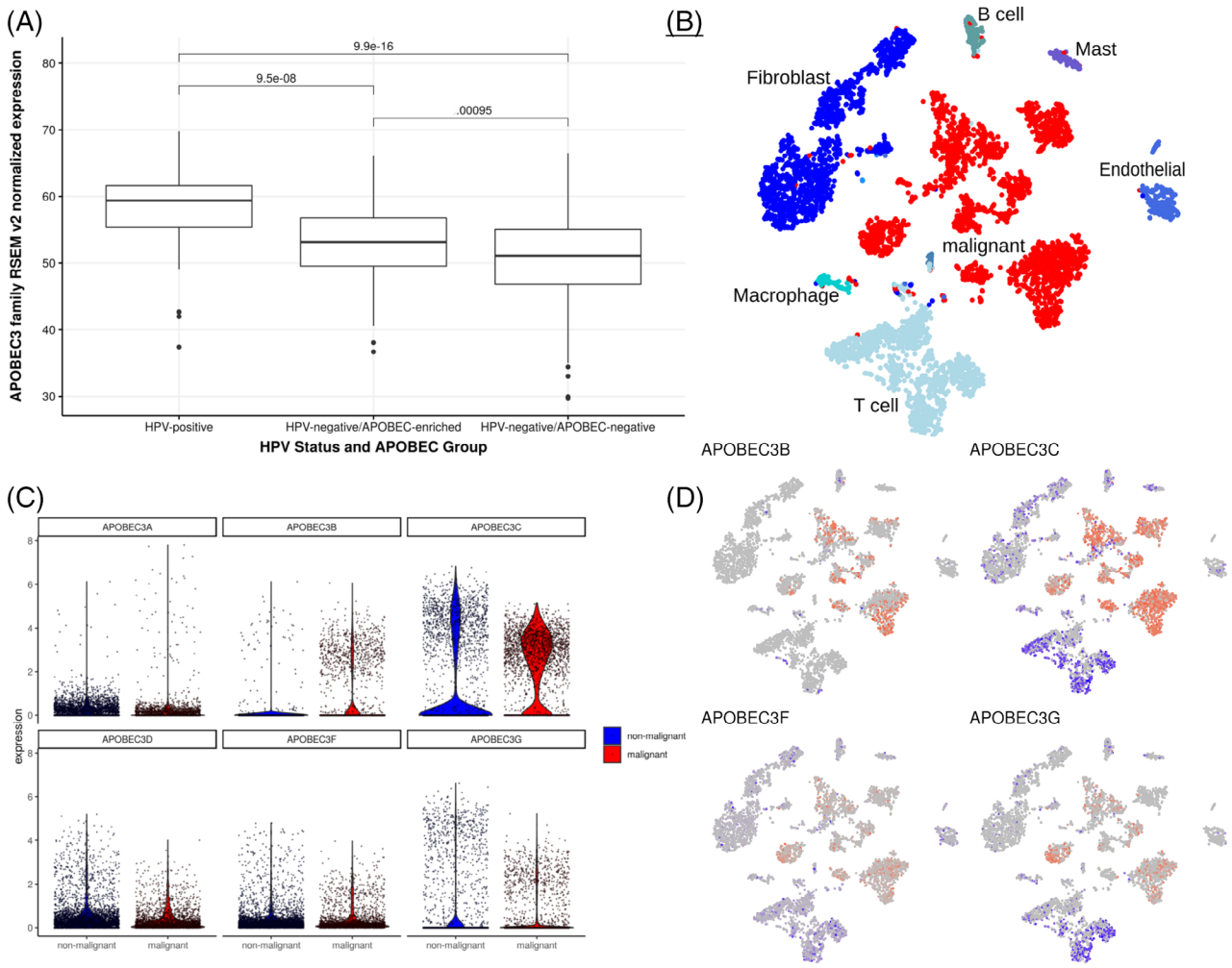

FIGURE 5 Independent single-cell expression data demonstrates the expression of APOBEC3C and APOBEC3B in tumor cells. A, Aggregated expression of APOBEC3 family genes for the three groups HPV-positive, HPV-negative/APOBEC-enriched, HPV-negative/APOBEC-negative. HPV-positive cases show significantly higher APOBEC3 expression than HPV-negative cases. Among those, the APOBEC-enriched subgroup exhibits significantly higher APOBEC3 gene expression. B, tSNE projection of all cells from 17 single-cell transcriptomics-profiled cases,[30] grouped into cell types. C, Violin plots of APOBEC3 gene expression between malignant (red) and nonmalignant cells (blue). APOBEC3B and APOBEC3C gene expression were detected in tumor cells. D, tSNE plots with projected expression of genes in the APOBEC3 family in 17 single-cell data sets of HPV-negative cases.[30] Biomarker-based groups of malignant (red) and nonmalignant cells (blue). Expression strength indicated by color intensity, with gray indicating that no expression was detected [Color figure can be viewed at wileyonlinelibrary.com]

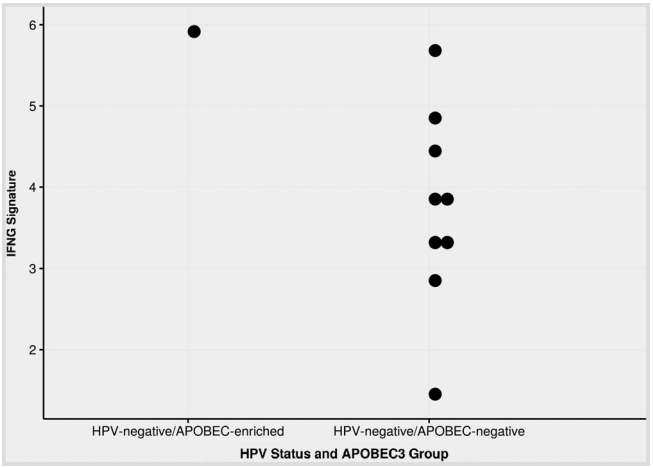

FIGURE 6 Independent analysis in a clinical cohort. IFNG signature score in the head-and-neck DKTK Master cohort grouped by APOBEC status for all HPV-negative cases. The only identified HPV-negative/APOBEC-enriched sample harbored the highest IFNG gene expression signature score

Among those, APOBEC3B and APOBEC3C gene expression were highest in malignant cells (Figure 5B-D).

3.6 | Independent validation of findings

In an independent cohort of 10 HPV-negative cases of HNSCC, sequenced for the DKTK MASTER program from six cancer centers in Germany, we set out to validate these findings. We identified one HPV-negative patient with an APOBEC-enriched mutational signature. Again, we computed the IFNG signature score and compared it between the already defined groups (Figure 6). The HPV-negative case with APOBEC enrichment (Figure S8, data available in Table S6) showed the highest inflammation in this cohort.

4 | DISCUSSION

Immune checkpoint inhibition has become an important treatment option in HNSCC, providing a benefit in a subset of patients.[35] The predictive value of a T-cell inflamed phenotype, as defined by an IFNG expression signature, has been shown in HNSCC and other tumor types.[3,4] Additionally, a high mutational load is correlated with response to immune checkpoint inhibition.[5] Yet, in our and other analyses, no clinically useful correlation between those two predictive markers was shown.[6]

To better understand differential immune activation and evasion in HNSCC, we analyzed the relationship between different mutational signatures and inflammation in HNSCC. An APOBEC-induced TCW mutational signature was significantly associated with a T-cell inflamed phenotype. This association could be validated in other tumor types, including lung and bladder cancer. Previous studies also support the role of APOBEC-induced mutational signatures in immune activation in several cancer types.[36,37] Among tumors with a high APOBEC mutational burden, Faden et al described HNSCC to have the highest IFNG levels, especially among HPV-positive cases.[38] In addition to these analyses, we show that, despite overall high levels of inflammation and APOBEC mutagenesis in HPV-positive HNSCC, a dose-dependent association between TCW mutations and inflammation is restricted to HPV-negative cases, thus leading to the establishment of an APOBEC-associated subgroup with differential immune activation among HPV-negative samples. We attribute the difference between HPV-positive and HPV-negative cases to the overall high impact of APOBEC-induced tumorigenesis in HPV-positive HNSCC[11] and a generally higher level of IFNG activation in these tumors. The activation of APOBEC in non-virally associated tumors has also been shown across cancer types.[14] This signature has been proposed to occur later in tumorigenesis and to induce branched evolution in lung cancer.[34,39]

Our own analyses in HNSCC rather suggest an early APOBEC activation in a subset of HPV-negative HNSCC with an immunogenic phenotype, thus proposing a different oncogenic mechanism in HNSCC, further supporting the idea of a distinct subgroup. It is currently unclear what drives this APOBEC activation. Previous analyses have suggested a link with single strand exposure and DNA repair defects.[40,41] It is also conceivable that short-term viral exposure induces APOBEC activation and carcinogenesis without genomic viral integration in some patients. Faden et al also suggested a potential role of germline APOBEC polymorphisms in mutagenesis.[38]

A subgroup of HPV-negative oral squamous cell carcinoma patients in never-smokers, never-drinkers with high tumor inflammation has been described in the literature.[42] This agrees with our observation, since smokers were underrepresented in the APOBEC-associated subgroup that was also enriched for tumors arising from the oral cavity. Further research focusing on the impact of short-term viral exposure and APOBEC-activation or virus-independent mechanisms of APOBEC-activation, especially in this hard-to-treat subgroup, are of interest.

We were not able to immunohistochemically analyze APOBEC protein expression in HNSCC and HNSCC patient-derived xenograft models, a well-known problem with currently available APOBEC3 antibodies.[12] In the TCGA data, APOBEC3A was most prominently expressed in the APOBEC-enriched subgroup. However, the tumor microenvironment poses a challenge in the analysis of bulk data. Inflammatory signatures, such as the IFNG signature, are associated with more immune infiltration and lower tumor purity. We therefore resorted to a re-analysis of publicly available single-cell gene expression data. Doing so, we were able to circumvent the bias of measuring APOBEC3 activity in the tumor microenvironment.[43] Here, expression of APOBEC3 subtypes 3B and 3C was most prominent among malignant cells. APOBEC3B has also been identified in previous publications on APOBEC activation in cancer, including HNSCC,[13,37] whereas the role of APOBEC3C remains less well defined. Since transient expression of APOBEC3 subtypes has been described,[44] short term activity of other APOBEC3-subtypes might cause mutations in the absence of APOBEC gene expression in later analyses, thus potentially explaining the observed differences. The observed different

contributions of APOBEC mutational Signatures 2 and 13 between HPV-positive and HPV-negative samples might also reflect different underlying APOBEC3-activity.

It is currently unclear what causes the T-cell inflamed phenotype in APOBEC-induced cancers. We were able to show that these tumors, despite harboring the same overall mutational load, show a distinct immune escape, represented by an enrichment for mutations in immunotherapy-essential genes (such as HLA-A), expression of regulatory immune signatures, including myeloid-derived, as well as expression of immune checkpoint molecules. Furthermore, these samples cluster in the immunogenic mesenchymal/inflamed subgroup.[8] It is possible that APOBEC-induced mutations are more prone to detection by the immune system, due to their association with viral infections. Yet, our own analyses in APOBEC-induced cancers did not show an increase in bioinformatically predicted neo-antigens (data not shown). Therefore, the reasons for the different mechanisms of immune evasion in APOBEC-associated HPV-negative HNSCC are not known but might also be relevant in other tumor types including urothelial[45,46] or lung cancer.[37] Does APOBEC-activity translate into differential response to immune checkpoint inhibition? Early studies suggest that APOBEC-associated tumors might indeed respond better to ICI therapy.[37,47] We were able to find some supporting evidence for the differential immune activation also within the recurrent/metastatic DKTK-MASTER cohort. However, this cohort is small and does not represent the demographics of the majority of HNSCC patients. Thus, further research is required to analyze this association, especially in patient cohorts treated with immune checkpoint inhibition. Mutational signatures inferred from DNA sequencing and specifically APOBEC3-associated motifs should be further investigated as a potentially predictive biomarker for immune checkpoint inhibition in HPV-negative HNSCC.

ACKNOWLEDGEMENTS

This work was funded by a grant awarded by Berliner Krebsgesellschaft e.V. to DTR, FK and DB. DTR is a participant in the Berlin Institute of Health - Charité Clinical Scientist Program funded by the Charité - Universitätsmedizin Berlin and the Berlin Institute of Health. The DKTK MASTER trial is funded by the German Cancer Consortium (DKTK). The results shown here are in part based upon data generated by the TCGA Research Network: http://cancergenome.nih.gov/

CONFLICT OF INTEREST

A. S. reports receiving research funding from Chugai, BMS, Ventana Roche and honoraria from Bayer, Novartis, BMS, AstraZeneca, Roche, Takeda, ThermoFisher, Illumina (Advisory Board) and Takeda, Roche, BMS, Illumina, AstraZeneca, Novartis, ThermoFisher, Bayer, MSD, Lilly (Speaker). W. W. reported honoraria unrelated to the current work (speaker's bureau and advisory board) from AstraZeneca, MSD, BMS, Bayer, Roche, Pfizer, Merck, Lilly, Novartis, Takeda, Amgen, Astellas and Research Funding from Bruker, MSD, BMS and Roche. The other authors report no potential conflict of interest that is relevant to this work.

DATA ACCESSIBILITY

Data sources and handling of the publicly available data used in our study are described in the Materials and Methods. The other data and further details are available from the corresponding author upon request.

ETHICS STATEMENT

The DKTK MASTER trial was approved by the local ethics committees. Written, informed consent was obtained from all participating patients.

ORCID

Clemens Messerschmidt https://orcid.org/0000-0001-8632-656X
Benedikt Obermayer https://orcid.org/0000-0002-9116-630X
Konrad Klinghammer https://orcid.org/0000-0001-6425-4833
Sebastian Ochsenreither https://orcid.org/0000-0001-6024-4312
Denise Treue https://orcid.org/0000-0002-0657-5505
Albrecht Stenzinger https://orcid.org/0000-0003-1001-103X
Stefan Fröhling https://orcid.org/0000-0001-7907-4595
Christian H. Brandts https://orcid.org/0000-0003-1732-2535
Ingeborg Tinhofer https://orcid.org/0000-0002-0512-549X
Ulrich Keilholz https://orcid.org/0000-0001-6773-9406
Dieter Beule https://orcid.org/0000-0002-3284-0632
Damian T. Rieke https://orcid.org/0000-0003-0027-7977

REFERENCES

1. Hanahan D, Weinberg RA. Hallmarks of cancer: the next generation. *Cell*. 2011;144:646-674.
2. Ferris RL, Blumenschein G, Fayette J, et al. Nivolumab for recurrent squamous-cell carcinoma of the head and neck. *N Engl J Med*. 2016;375:1856-1867.
3. Seiwert TY, Burtness B, Mehra R, et al. Safety and clinical activity of pembrolizumab for treatment of recurrent or metastatic squamous cell carcinoma of the head and neck (KEYNOTE-012): an open-label, multicentre, phase 1b trial. *Lancet Oncol*. 2016;17:956-965.
4. Ayers M, Lunceford J, Nebozhyn M, et al. IFN-γ-related mRNA profile predicts clinical response to PD-1 blockade. *J Clin Invest*. 2017;127:2930-2940.
5. van Allen EM, Miao D, Schilling B, et al. Genomic correlates of response to CTLA-4 blockade in metastatic melanoma. *Science (80-)*. 2015;350:207-211.
6. Cristescu R, Mogg R, Ayers M, et al. Pan-tumor genomic biomarkers for PD-1 checkpoint blockade–based immunotherapy. *Science (80-)*. 2018;362:eaar3593.
7. Rieke DT, Klinghammer K, Keilholz U. Targeted therapy of head and neck cancer. *Oncol Res Treat*. 2016;39:780-786.
8. Keck MK, Zuo Z, Khattri A, et al. Integrative analysis of head and neck cancer identifies two biologically distinct HPV and three non-HPV subtypes. *Clin Cancer Res*. 2015;21:870-881.
9. Mehra R, Seiwert TY, Gupta S, et al. Efficacy and safety of pembrolizumab in recurrent/metastatic head and neck squamous cell carcinoma: pooled analyses after long-term follow-up in KEYNOTE-012. *Br J Cancer*. 2018;119:153-159.
10. Blank CU, Haanen JB, Ribas A, Schumacher TN. The cancer immunogram. *Science (80-)*. 2016;352:658-660.
11. Henderson S, Chakravarthy A, Su X, Boshoff C, Fenton TR. APOBEC-mediated cytosine deamination links PIK3CA helical domain mutations to human papillomavirus-driven tumor development. *Cell Rep*. 2014;7(6):1833-1841. https://doi.org/10.1016/j.celrep.2014.05.012

12. Venkatesan S, Rosenthal R, Kanu N, et al. Perspective: APOBEC mutagenesis in drug resistance and immune escape in HIV and cancer evolution. *Ann Oncol*. 2018;29:563-572.
13. Burns MB, Temiz NA, Harris RS. Evidence for APOBEC3B mutagenesis in multiple human cancers. *Nat Genet*. 2013;45:977-983.
14. Alexandrov LB, Nik-Zainal S, Wedge DC, et al. Signatures of mutational processes in human cancer. *Nature*. 2013;500:415-421.
15. Lawrence MS, Sougnez C, Lichtenstein L, et al. Comprehensive genomic characterization of head and neck squamous cell carcinomas. *Nature*. 2015;517:576-582.
16. Collisson EA, Campbell JD, Brooks AN, et al. Comprehensive molecular profiling of lung adenocarcinoma. *Nature*. 2014;511:543-550.
17. Weinstein JN, Akbani R, Broom BM, et al. Comprehensive molecular characterization of urothelial bladder carcinoma. *Nature*. 2014;507 (7492):315-322. https://doi.org/10.1038/nature12965
18. Hammerman PS, Voet D, Lawrence MS, et al. Comprehensive genomic characterization of squamous cell lung cancers. *Nature*. 2012; 489:519-525.
19. Roberts SA, Lawrence MS, Klimczak LJ, et al. An APOBEC cytidine deaminase mutagenesis pattern is widespread in human cancers. *Nat Genet*. 2013;45:970-976.
20. Huang PJ, Chiu LY, Lee CC, et al. MSignatureDB: a database for deciphering mutational signatures in human cancers. *Nucleic Acids Res*. 2018;46(D1):D964-D970. https://doi.org/10.1093/nar/gkx1133
21. Buitrago-Pérez A, Garaulet G, Vázquez-Carballo A, Paramio JM, García-Escudero R. Molecular signature of HPV-induced carcinogenesis: pRb, p53 and gene expression profiling. *Curr Genomics*. 2009;10: 26-34.
22. Tang K-W, Alaei-Mahabadi B, Samuelsson T, Lindh M, Larsson E. The landscape of viral expression and host gene fusion and adaptation in human cancer. *Nat Commun*. 2013;4:2513.
23. Gao J, Aksoy BA, Dogrusoz U, et al. Integrative analysis of complex cancer genomics and clinical profiles using the cBioPortal. *Sci Signal*. 2013;6:pl1-pl1.
24. Charoentong P, Finotello F, Angelova M, et al. Pan-cancer Immunogenomic analyses reveal genotype-Immunophenotype relationships and predictors of response to checkpoint blockade. *Cell Rep*. 2017;18: 248-262.
25. Hänzelmann S, Castelo R, Guinney J. GSVA: gene set variation analysis for microarray and RNA-Seq data. *BMC Bioinformatics*. 2013;14:7. https://doi.org/10.1186/1471-2105-14-7
26. Ritchie ME, Phipson B, Wu D, et al. Limma powers differential expression analyses for RNA-sequencing and microarray studies. *Nucleic Acids Res*. 2015;43(7):e47. https://doi.org/10.1093/nar/gkv007
27. Patel SJ, Sanjana NE, Kishton RJ, et al. Identification of essential genes for cancer immunotherapy. *Nature*. 2017;548:537-542.
28. Jäger M, Wang K, Bauer S, Smedley D, Krawitz P, Robinson PN. Jannovar: a Java library for exome annotation. *Hum Mutat*. 2014;35: 548-555.
29. Storey J. qvalue: Q-Value estimation for false discovery rate control. R package version 2.0.0. 2015. DOI: https://doi.org/10.18129/B9.bioc.qvalue
30. Puram SV, Tirosh I, Parikh AS, et al. Single-cell transcriptomic analysis of primary and metastatic tumor ecosystems in head and neck cancer. *Cell*. 2017;171:1611-1624.e24.
31. Butler A, Hoffman P, Smibert P, Papalexi E, Satija R. Integrating single-cell transcriptomic data across different conditions, technologies, and species. *Nat Biotechnol*. 2018;36:411-420.
32. Patro R, Duggal G, Love MI, Irizarry RA, Kingsford C. Salmon provides fast and bias-aware quantification of transcript expression. *Nat Methods*. 2017;14:417-419.
33. Chow LQM, Mehra R, Haddad RI, et al. Biomarkers and response to pembrolizumab (pembro) in recurrent/metastatic head and neck squamous cell carcinoma (R/M HNSCC). *J Clin Oncol*. 2016;34:6010-6010.
34. McGranahan N, Favero F, de Bruin EC, Birkbak NJ, Szallasi Z, Swanton C. Clonal status of actionable driver events and the timing of mutational processes in cancer evolution. *Sci Transl Med*. 2015;7:283ra54.
35. Burtness B, Harrington KJ, , , et al. KEYNOTE-048: phase III study of first-line pembrolizumab (P) for recurrent/metastatic head and neck squamous cell carcinoma (R/M HNSCC). *Ann Oncol*. 2018;29(Suppl. 8):viii729–viii729. https://doi.org/10.1093/annonc/mdy424.045
36. Budczies J, Seidel A, Christopoulos P, et al. Integrated analysis of the immunological and genetic status in and across cancer types: impact of mutational signatures beyond tumor mutational burden. *Oncoimmunology*. 2018;7:e1526613. https://doi.org/10.1080/2162402X.2018.1526613
37. Wang S, Jia M, He Z, Liu X-S. APOBEC3B and APOBEC mutational signature as potential predictive markers for immunotherapy response in non-small cell lung cancer. *Oncogene*. 2018;37:3924-3936.
38. Faden DL, Ding F, Lin Y, et al. APOBEC mutagenesis is tightly linked to the immune landscape and immunotherapy biomarkers in head and neck squamous cell carcinoma. *Oral Oncol*. 2019;96:140-147.
39. Swanton C, McGranahan N, Starrett GJ, Harris RS. APOBEC enzymes: mutagenic fuel for cancer evolution and heterogeneity. *Cancer Discov*. 2015;5:704-712.
40. Chen J, Miller BF, Furano AV. Repair of naturally occurring mismatches can induce mutations in flanking DNA. *Elife*. 2014;3:e02001. https://doi.org/10.7554/eLife.02001
41. Taylor BJ, Nik-Zainal S, Wu YL, et al. DNA deaminases induce break-associated mutation showers with implication of APOBEC3B and 3A in breast cancer kataegis. *Elife*. 2013;2:e00534. https://doi.org/10.7554/eLife.00534
42. Foy J-P, Bertolus C, Michallet M-C, et al. The immune microenvironment of HPV-negative oral squamous cell carcinoma from never-smokers and never-drinkers patients suggests higher clinical benefit of IDO1 and PD1/PD-L1 blockade. *Ann Oncol*. 2017;28:1934-1941.
43. Leonard B, Starrett GJ, Maurer MJ, et al. APOBEC3G expression correlates with T-cell infiltration and improved clinical outcomes in high-grade serous ovarian carcinoma. *Clin Cancer Res*. 2016;22:4746-4755.
44. Petljak M, Alexandrov LB, Brammeld JS, et al. Characterizing mutational signatures in human cancer cell lines reveals episodic APOBEC mutagenesis. *Cell*. 2019;176:1282-1294.e20. https://doi.org/10.1016/j.cell.2019.02.012
45. Mullane SA, Werner L, Rosenberg J, et al. Correlation of Apobec Mrna expression with overall survival and pd-l1 expression in urothelial carcinoma. *Sci Rep*. 2016;6:27702.
46. Glaser AP, Fantini D, Wang Y, et al. APOBEC-mediated mutagenesis in urothelial carcinoma is associated with improved survival, mutations in DNA damage response genes, and immune response. *Oncotarget*. 2018;9:4537-4548.
47. Miao D, Margolis CA, Vokes NI, et al. Genomic correlates of response to immune checkpoint blockade in microsatellite-stable solid tumors. *Nat Genet*. 2018;50:1271-1281.

SUPPORTING INFORMATION

Additional supporting information may be found online in the Supporting Information section at the end of this article.

How to cite this article: Messerschmidt C, Obermayer B, Klinghammer K, et al. Distinct immune evasion in APOBEC-enriched, HPV-negative HNSCC. *Int. J. Cancer*. 2020;147:2293–2302. https://doi.org/10.1002/ijc.33123